Available online at www.sciencedirect.com
ScienceDirect
Journal of Hazardous Materials 154 (2008) 639–648
Journal of Hazardous Materials
www.elsevier.com/locate/jhazmat

Sorption kinetics and isotherm studies of a cationic dye using agricultural waste: Broad bean peels

B.H. Hameed [a,*], M.I. El-Khaiary [b]

[a] School of Chemical Engineering, Engineering Campus, Universiti Sains Malaysia, 14300 Nibong Tebal, Penang, Malaysia
[b] Chemical Engineering Department, Faculty of Engineering, Alexandria University, El-Hadara, Alexandria 21544, Egypt

Received 21 August 2007; received in revised form 19 October 2007; accepted 22 October 2007
Available online 30 October 2007

Abstract

In this paper, broad bean peels (BBP), an agricultural waste, was evaluated for its ability to remove cationic dye (methylene blue) from aqueous solutions. Batch mode experiments were conducted at 30 °C. Equilibrium sorption isotherms and kinetics were investigated. The kinetic data obtained at different concentrations have been analyzed using pseudo-first-order, pseudo-second-order and intraparticle diffusion equations. The experimental data fitted very well the pseudo-first-order kinetic model. Analysis of the temportal change of q indicates that at the beginning of the process the overall rate of adsorption is controlled by film-diffusion, then at later stage intraparticle-diffusion controls the rate. Diffusion coefficients and times of transition from film to pore-diffusion control were estimated by piecewise linear regression. The experimental data were analyzed by the Langmuir and Freundlich models. The sorption isotherm data fitted well to Langmuir isotherm and the monolayer adsorption capacity was found to be 192.7 mg/g and the equilibrium adsorption constant K_a is 0.07145 l/mg at 30 °C. The results revealed that BBP was a promising sorbent for the removal of methylene blue from aqueous solutions.

Keywords: Broad bean peel; Methylene blue; Adsorption isotherm; Equilibrium; Kinetics

1. Introduction

Synthetic dyestuffs are used extensively in textile, paper, printing and other industries. Dyes are classified as follows: anionic—direct, acid and reactive dyes; cationic—basic dyes; non-ionic—disperse dyes [1,2]. Basic dyes have high brilliance and intensity of colors and are highly visible even in a very low concentration [2–7]. It is reported that there are over 100,000 commercially available dyes with a production of over 7×10^5 metric tonnes per year [3,8]. Dyes may significantly affect photosynthetic activity in aquatic life due to reduced light penetration and may also be toxic to some aquatic life due to the presence of aromatics, metals, chlorides, etc. in them [1–4,8,9].

A wide range of methods has been developed for the removal of synthetic dyes from waters and wastewaters to decrease their impact on the environment. The technologies involve adsorption on inorganic or organic matrices, decolorization by photocatalysis, and/or by oxidation processes, microbiological or enzymatic decomposition, etc. [10]. Adsorption has been shown to be the most promising option for the removal of non-biodegradable organics from aqueous streams, activated carbons being the most common adsorbent for this process due to their effectiveness and versatility.

Activated carbon as an adsorbent has been widely investigated for the adsorption of basic dyes [11–15], but its high-cost limits its commercial application. In recent years, extensive research has been undertaken to develop alternative and economic adsorbents.

An economic sorbent is defined as one which is abundant in nature, or is a by-product or waste from industry and requires little processing [16]. The use of unconventional adsorbents has the following features: (1) it can be obtained abundant locally and cheaply. Most of them are readily utilized; (2) regeneration of these low-cost substitutes is not necessary whereas regeneration of activated carbon is essential. Such regeneration may result in additional effluent and the adsorbent may suffer a considerable loss; (3) less operation cost in terms of maintenance and supervision are required for the unconventional adsorption systems; (4)

* Corresponding author. Fax: +60 4 594 1013.
E-mail address: chbassim@eng.usm.my (B.H. Hameed).

0304-3894/$ – see front matter © 2007 Elsevier B.V. All rights reserved.
doi:10.1016/j.jhazmat.2007.10.081

utilization of industrial solid waste for the treatment of industrial wastewater is helpful not only to the environment, but also to reduce the disposal cost [17]. Such alternatives include palm ash and chitosan/oil palm ash [18,19], shale oil ash [20], *Posidonia oceanica* (L.) fibres [21] palm kernel fibre [22], sand [23] and water-hyacinth [24].

In this work, we attempt to use broad bean (*Vicia faba* L.) peels as an alternative low-cost sorbent in the removal of methylene blue from aqueous solutions. Broad beans are extensively grown in different parts of the world and, in particular, in the Mediterranean region [25]. Broad bean can be used as a dietary item alone or can serve as potential supplement to cereal diets, especially for the preparation of inexpensive protein-rich food for children [26]. It contains 25.2% of proteins, 46.5% of carbohydrates, 1.5% of lipids and 10.3% of dietary fibre [27]. Broad beans are usually available throughout the year as fresh, frozen and fully mature. Due to the high consumption of broad beans, massive amounts of the peels (as waste) are disposed, causing a severe problem in the community. In the interest of the environment, we utilized this agricultural waste as a low-cost sorbent to remove basic dye from aqueous solutions.

The objective of our investigation was to investigate the potential of broad bean peels (BBP), an agricultural solid waste, as low-cost sorbent in the removal of the cationic dye, methylene blue, from aqueous solutions. The equilibrium and kinetics of the process were modeled by conventional theoretical methods. In order to gain insight into the dynamics of the process, the mechanism controlling the rate of adsorption was also studied.

2. Materials and methods

2.1. Sorbate

The cationic dye used in this study was methylene blue (MB) purchased from Sigma–Aldrich. The MB was chosen in this study because of its known strong adsorption onto solids. MB has a chemical formula of $C_{16}H_{18}N_3SCl$. The maximum wavelength of this dye is 668 nm. The structure of MB is shown as follows (Scheme 1):

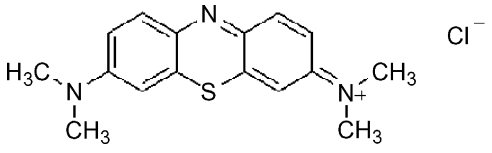

Scheme 1. Chemical structure of methylene blue.

2.2. Sorbent

Dried broad beans seeds were purchased from a local market. The seeds were first soaked in distilled water for a few hours and then boiled for 30 min to make them easier to peel. Then they were manually peeled. Collected peels were boiled for 10 min to remove the surface adhered particles. Peels were then washed with distilled water to remove the surface adhered particles and water soluble materials, chopped to ca. 4–6 mm and oven-dried at 60 °C for 48 h. The dried sample was ground and sieved to obtain a particle size range of 350–400 μm and stored in plastic bottle for further use. No other chemical or physical treatments were used prior to adsorption experiments.

Scanning electron microscopy (SEM) (ZEISS SUPRA 35 VP) analysis was carried out on the BBP to study its surface texture before and after adsorption.

2.3. Equilibrium studies

Sorption experiments were carried out by adding a fixed amount of BBP sorbent (0.30 g) into a number of 250 ml-stoppered glass Erlenmeyers flasks containing a definite volume (200 ml in each case) of different initial concentrations (30–325 mg/l) of dye solution at pH 5 and temperature 30 °C. The flasks were placed in a thermostatic water-bath shaker and agitation was provided at 130 rpm for 320 min to ensure equilibrium was reached. Aqueous samples were taken from the solutions and the concentrations were analyzed. At time $t = 0$ and equilibrium, the dye concentrations were measured by a double beam UV/Vis spectrophotometer (UV-1601, Shimadzu) at 668 nm.

The amount of sorption at equilibrium, q_e (mg/g), was calculated by:

$$q_e = \frac{(C_0 - C_e)V}{W} \quad (1)$$

where C_0 and C_e (mg/l) are the liquid-phase concentrations of dye at initial and equilibrium, respectively. V is the volume of the solution (l) and W is the mass of dry sorbent used (g).

2.4. Effect of solution pH

The effect of pH on the amount of dye removal was studied over the pH range from 2 to 10. In this study, 200 ml of dye solution of 60 mg/l at different pH values (2–10) was agitated with 0.3 g of BBP using water-bath shaker at 30 °C. Agitation was made at 130 rpm for 320 min, which was more than sufficient time to reach equilibrium at a constant agitation speed of 130 rpm. The pH was adjusted with 0.1 N NaOH and 0.1 N HCl solutions and measured by using a pH meter (Ecoscan, EUTECH Instruments, Singapore).

2.5. Batch kinetic studies

The procedures of kinetic experiments were basically identical to those of equilibrium tests. The aqueous samples were taken at preset time intervals, and the concentrations of dye were similarly measured. All the kinetic experiments were carried out at pH 5. The amount of sorption at time t, q_t (mg/g), was calculated by:

$$q_t = \frac{(C_0 - C_t)V}{W} \quad (2)$$

where C_t (mg/l) is the liquid-phase concentrations of dye at any time.

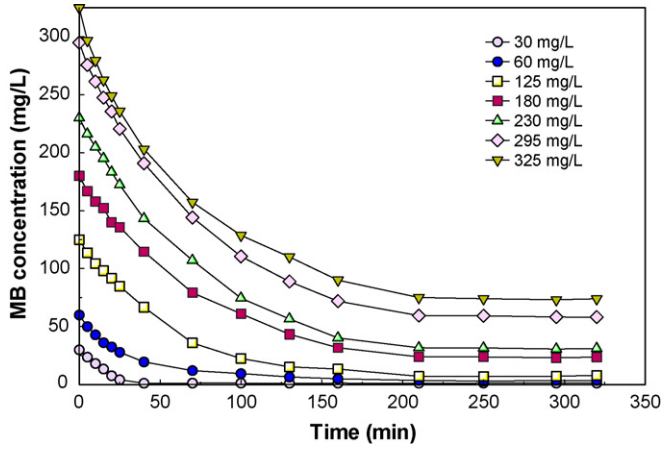

Fig. 1. The sorption of MB on BBP for different initial concentrations at 30 °C and BBP dose 1.5 g/l.

3. Results and discussion

3.1. Kinetic study

Fig. 1 shows the effect of initial methylene blue concentration, C_o, on the kinetics of dye sorption at BBP dosage 1.5 g/l and 30 °C. An increase in the initial MB concentration leads to a decrease in the MB removal. As the initial MB concentration increases from 30 to 325 mg/l, the equilibrium removal of MB decreases from 95.7% to 77.2%. It is also noticed in Fig. 1 that increasing C_o leads to an increase in the time needed to reach equilibrium from about 40 min to 200 min when C_o increases from 30 to 325 mg/l.

The modeling of the system's transient behavior at different initial MB concentrations was studied using the Lagergren's pseudo-first-order [28] and Ho's pseudo-second-order models [29]. The Lagergren equation, a pseudo-first-order equation, models the kinetics of adsorption process as follows:

$$\frac{dq}{dt} = k_1(q_e - q) \tag{3}$$

where q_e is the amount of adsorbate adsorbed at equilibrium (mg/g), q is the amount of adsorbate adsorbed at time t (mg/g) and k_1 is the rate constant of pseudo-first-order adsorption (min^{-1}). Since $q = 0$ at $t = 0$, the initial rate of adsorption can be calculated from Eq. (4) as follows:

$$h_{o,1} = k_1 q_e \tag{4}$$

By integration of Eq. (3) for the boundary conditions $t = 0$ to $t = t$ and $q = 0$ to $q = q_e$, gives:

$$q = q_e(1 - e^{-k_1 t}) \tag{5}$$

On the other hand, the pseudo-second-order kinetic equation of Ho is expressed in the form:

$$\frac{dq}{dt} = k_2(q_e - q)^2 \tag{6}$$

where k_2 is the rate constant of pseudo-second-order adsorption (g/mg min) and q_e is the amount of solute adsorbed at equilibrium (mg/g). The integration of Eq. (6) for boundary conditions $t = 0$ to $t = t$ and $q = 0$ to $q = q$ gives:

$$q = \frac{q_e^2 k_2 t}{1 + q_e k_2 t} \tag{7}$$

and the initial rate of adsorption $h_{o,2}$ is:

$$h_{o,2} = k_2 q_e^2 \tag{8}$$

The experimental results of the dye uptake, q, versus time were fitted to both models by the method of nonlinear regression using the software package NCSS [30]. The regression results are presented in Table 1 and Figs. 2 and 3. It can be seen from the plots of q versus t that an increase in initial MB concentration leads to an increase in the adsorption capacity, q_e. As the initial MB concentration increases from 30 to 325 mg/l, the experimentally observed sorption capacity, q_{exp}, increases from 19.15 to 167.52 mg/g. It is observed from Fig. 2 that for all initial MB concentrations, the adsorption data were well represented by Lagergren's model of Eq. (5) for the entire period of adsorption. The values of sorption capacity, q_e, calculated from Lagergren's model are also close to the values observed experimentally, q_{exp}. The values of the coefficient of determination, R^2, are in the range 0.9829–0.9993.

The kinetic data was also fitted to the pseudo-second-order model of Eq. (7). By comparing Figs. 2 and 3, it is obvious that Lagergren's model fits the experimental data better than the pseudo-second-order model for the entire adsorption period. Also, from the regression results in Table 1, the values of q_e obtained from Lagergeren's model are very close to

Table 1
Pseudo-first-order and pseudo-second-order rate constants at 30 °C and different initial MB concentrations (C_o: mg/l; q_e: mg/g; h_o: mg/g min; k_1: min^{-1}; k_2: g/mg min)

Pseudo-first-order model						Pseudo-second-order-model			
C_o	q_{exp}	q_e	k_1	$h_{o,1}$	R^2	q_e	k_2	$h_{o,2}$	R^2
30	19.15	19.38	0.06459	1.251	0.9829	20.83	0.004463	1.936	0.9422
60	37.71	36.85	0.03419	1.260	0.9944	41.59	0.001007	1.742	0.9975
125	78.44	79.97	0.01787	1.429	0.9978	97.31	0.0001873	1.774	0.9871
180	104.24	107.87	0.01373	1.481	0.9983	136.95	9.512×10^{-5}	1.784	0.9918
230	132.47	137.45	0.01364	1.875	0.9984	175.03	7.332×10^{-5}	2.246	0.9901
295	157.69	161.80	0.01438	2.327	0.9993	203.51	6.848×10^{-5}	3.512	0.9938
325	167.52	168.13	0.01651	2.776	0.9967	205.57	8.343×10^{-5}	3.526	0.9972

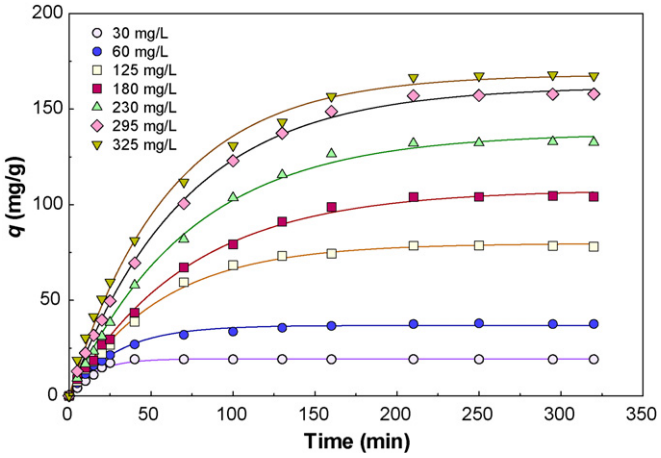

Fig. 2. The fitting of Lagergren's model for MB on BBP for different initial concentrations at 30 °C and BBP dose 1.5 g/l.

the experimental results, while q_e values predicted from the pseudo-second-order model are always overestimated with the error in predicting q_e increasing at higher initial MB concentration. By comparing the coefficient of determination, R^2, in Table 1, it is seen that except for the case of initial MB concentrations of 60 and 325 mg/l, the pseudo-second-order model fits the experimental results with lower R^2 values (0.9422–0.9938) than Lagergren's model (R^2 from 0.9829–0.9993). The higher R^2 values and the accurate estimations of q_e indicate that the adsorption kinetics are represented better by Lagergeren's model. The kinetic results reported for other adsorption systems show that the pseudo-second-order represents the experimental data adequately in many cases [11–13,18,21] but still there are cases where both the pseudo-first and pseudo-second-order models can represent the experimental data [24]. The present study is one of the few cases in which the pseudo-first order model is better. It is not known until now what are the properties of the adsorption system that makes it better represented by one model than the other. However, it is generally accepted that for most of the adsorption period the rate is controlled by various diffusion regimes, and therefore, the pseudo kinetic models are better considered as empirical equations that do not reflect the actual chemical and physical phenomena taking place. With that in mind, the pseudo kinetic models are still valuable as simple equations that predict the kinetics of adsorption systems and can be used in the design of adsorption units.

The relatively high R^2 values for the regression to the pseudo-second-order model for C_o values of 60 and 325 mg/l are caused by a good fit to the experimental results in the initial period of adsorption as seen in Fig. 4. Fig. 4 shows that in the initial period of adsorption (first 40 min), Lagergren's model fits the experimental data well for all initial MB concentrations except 60 and 325 mg/l, the adsorption results of these two concentrations are fitted better by the pseudo-second-order model in the initial adsorption period. However, as the adsorption time period increases, the pseudo-second-order model deviates from the data and the predicted values of q_e are largely overestimated.

It is also observed in Table 1 that when the MB initial concentration varies from 30 to 230 mg/l, the rate constant, k_1, decreases from 0.06459 to 0.01364 (mg/g min), but further increase in initial concentration to 325 mg/l causes k_1 to reverse the trend and increase to 0.01651. The nonlinear relationships between initial MB concentration and the rate constant suggests that more than one mechanism play roles in the sorption process, such as ion exchange, chelation and physical adsorption. The values of the initial sorption rate, $h_{o,1}$, are also shown in Table 1. When the initial MB concentration varies from 30 to 325 mg/l, values of $h_{o,1}$ increase from 1.251 to 2.776 mg/g min. This is due to the increasing driving force at higher MB concentrations.

Since the above calculations show that Lagergeren's model is better in predicting the adsorption kinetics at 30 °C and different values of C_o, the values of $q_{e,1}$ (at equilibrium) and q (at any

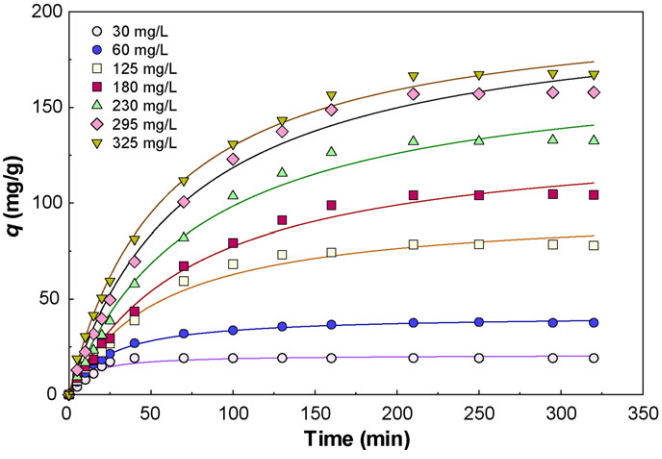

Fig. 3. The fitting of pseudo-second-order model for MB on BBP for different initial concentrations at 30 °C and BBP dose 1.5 g/l.

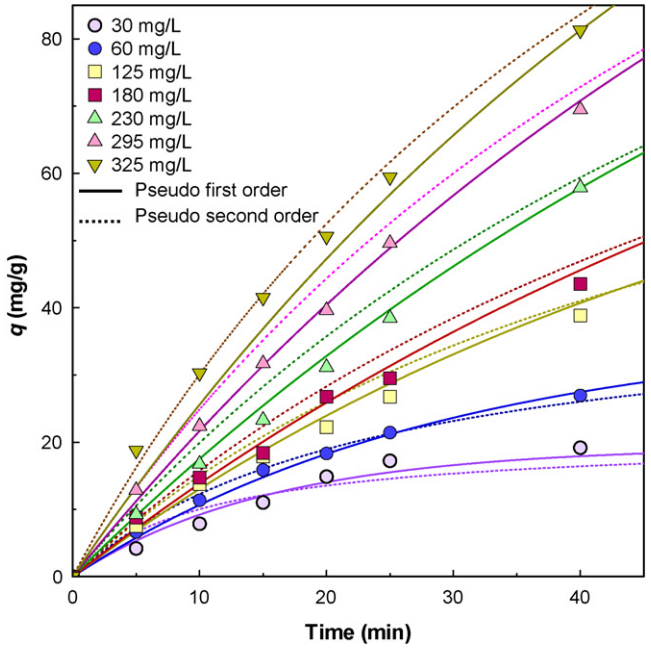

Fig. 4. The fitting of pseudo-second-order model for the initial period of adsorption of MB on BBP for different initial concentrations at 30 °C and BBP dose 1.5 g/l.

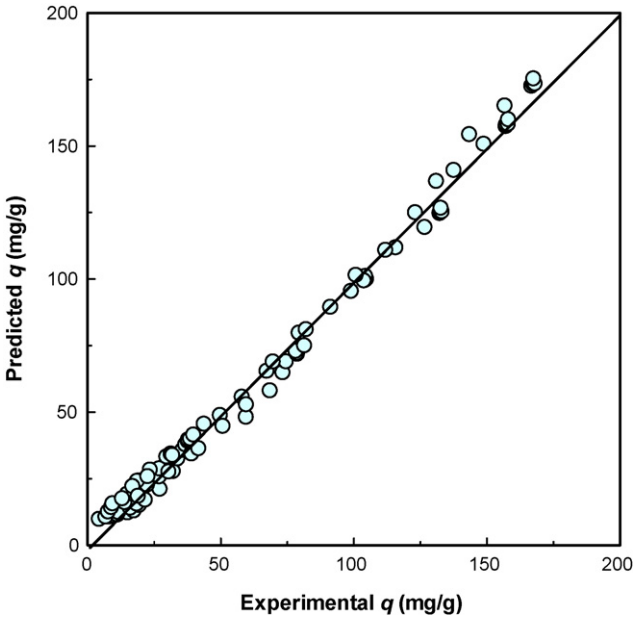

Fig. 5. Plot of experimentally determined q_e vs. values of q_e predicted from Eq. (8).

time) were correlated with the initial MB concentration to obtain expressions for these values in terms of C_o by multiple regression using the forward-addition method, the resulting empirical equations are:

$$q_{e,1} = 0.7088\ C_o - 0.0005620\ C_o^2 \quad (R^2 = 0.9978) \tag{9}$$

$$q = 9.0936 + 0.005974 C_o t - 2.3466 \times 10^{-5} C_o t^2 + 3.0607 \times 10^{-8} C_o t^3 \quad (R^2 = 0.9914) \tag{10}$$

Eq. (9) can be used to predict the equilibrium dye uptake for any C_o and BBP dose 1.5 g/l, and Eq. (10) can be used to predict the amount of MB adsorbed for any given C_o and contact time, and BBP dose 1.5 g/l. The predicted and experimental values of q at different times and initial MB concentrations are plotted in Fig. 5.

3.2. Sorption mechanism

The kinetic studies help in predicting the progress of adsorption, but the determination of the adsorption mechanism is also important for design purposes. In a solid–liquid adsorption process, the transfer of the adsorbate is controlled by either boundary layer diffusion (external mass transfer) or intraparticle diffusion (mass transfer through the pores), or by both. It is generally accepted that the adsorption dynamics consists of three consecutive steps:

- Transport of adsorbate molecules from the bulk solution to the external surface of the adsorbent by diffusion through the liquid boundary layer.
- Diffusion of the adsorbate from the external surface and into the pores of the adsorbent.
- Adsorption of the adsorbate on the active sites on the internal surface of the pores.

The last step, adsorption, is usually very rapid in comparison to the first two steps. Therefore, the overall rate of adsorption is controlled by either film or intraparticle diffusion, or a combination of both. Many studies have shown that the boundary layer diffusion is the rate controlling step in systems characterized by dilute concentrations of adsorbate, poor mixing, and small particle size of adsorbent. Whereas the intraparticle diffusion controls the rate of adsorption in systems characterized by high concentrations of adsorbate, good mixing, and big particle size of adsorbent [31]. Also, it has been noticed in many studies that boundary layer diffusion is dominant during the initial adsorbate uptake, then gradually the adsorption rate becomes controlled by intraparticle diffusion after the adsorbent's external surface is loaded with the adsorbate.

The intraparticle diffusion parameter, k_i (mg/g min$^{0.5}$) is defined by the following equation [32]:

$$q = k_i t^{0.5} + c \tag{11}$$

where q is the amount of MB adsorbed (mg/g) at time t, k_i is intraparticle diffusion constant (mg/g min$^{0.5}$), and c is the intercept. Theoretically, the plot of k_i versus $t^{0.5}$ should show at least four linear regions that represent boundary layer diffusion, followed by intraparticle diffusion in macro, meso, and micro pores [33]. These four regions are followed by a horizontal line representing the system at equilibrium.

The intraparticle diffusion plots of the experimental results, q versus $t^{0.5}$ for different initial MB concentrations at 30 °C and BBP dose of 1.5 g/l are shown in Fig. 6. From the figure it is observed that there are three linear regions. At the beginning of adsorption there is a linear region representing the rapid surface loading, followed by the second linear region representing pore diffusion, and finally a horizontal linear region representing equilibrium. The software package NCSS was used to apply the method of piecewise linear regression to avoid subjective judgment in choosing the beginning and end of each region. The results of piecewise linear regression are shown in Table 2 and

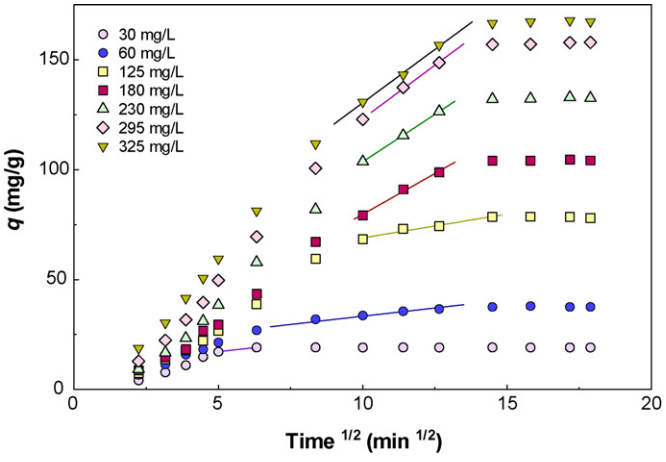

Fig. 6. Intraparticle diffusion plot for the adsorption at 30 °C and different initial MB concentrations (BBP dose: 1.5 g/l).

Table 2
Diffusion coefficients for sorption of MB on BBP at 30 °C, and different initial concentrations (C_o: mg/l; c: mg/g; k_i: mg/g min$^{0.5}$; k_s: min^{-1}; D_i: cm^2/s)

C_o	k_s	$D_i \times 10^6$	Film-diffusion period[a]	c	k_i	Pore diffusion period[b]
30	0.04231	9.538	0–16	9.914	1.465	25–40
60	0.02949	5.606	0–45	18.38	1.497	46–182
125	0.01392	2.945	0–37	47.31	2.167	102–219
180	0.01054	2.447	0–100	5.501	7.420	94–169
230	0.01143	2.392	0–80	10.30	8.627	100–175
295	0.01097	2.577	0–120	33.86	9.079	105–183
325	0.01215	2.654	0–149	33.57	9.709	81–190

[a] Estimated from the end of film-diffusion period according to Boyd's equation.
[b] Estimated from the second linear portion according to the pore-diffusion model.

the lines representing intraparticle diffusion are plotted in Fig. 6. It is observed that the time elapsed until pore diffusion starts controlling the rate of adsorption increases from 25 to 102 min when the initial MB concentration increases from 30 to 125 mg/l, but on further increase of initial MB concentration above 125 mg/l the elapsed time to the start of diffusion control does not change significantly. The intraparticle diffusion parameter, k_i, is determined from the slope of the second linear region while the intercept is proportional to the boundary layer thickness (or resistance). The calculated values of k_i and the intercept are shown in Table 2. It is obvious that values of k_i increase sharply from 1.465 to 7.420 mg/g min$^{0.5}$ when the initial MB concentration is increased from 30 to 180 mg/l. Further increase in the initial MB concentration from 180 to 325 mg/l has little effect on k_i raising its value to 9.709 mg/g min$^{0.5}$. It is also observed that the value of the intercept increases from 9.914 to 47.31 when C_o is increased from 30 to 125 mg/l, which indicates that the thickness (or the resistance to mass transfer) of the boundary layer increases significantly with increase of C_o in this range. However, on further increase of C_o to 180 mg/l the values of the intercept drops to 5.501 indicating a decrease in the resistance to mass transfer in the external boundary layer, and eventually the intercept value rises to 33.57 at C_o of 325 mg/l. This could be related to the aggregation behavior of MB molecules which are known to form dimmers and aggregates depending on the conditions of solution such as pH, concentration, temperature, and presence of other ions [34,35]. MB aggregates can migrate from the external surface of BBP to the internal pores, resulting in deaggregation of the MB aggregates and restoring monomers. At high loading rates of MB, it is expected that agglomerates are predominant in solution, while monomers and dimmers are virtually absent in the MB-adsorbent complexes on the solid surface.

The rate constants of external mass transfer were calculated using the plot of C/C_o against time at different initial MB concentrations (figure not shown). The experimental results were fitted to second order polynomials, then the slopes were calculated from the first derivative of the polynomial functions at $t = 0$. The values of initial adsorption rates, k_s (min^{-1}) are plotted in Fig. 7. It is observed that the rate in the initial period of adsorption, where external mass transfer is assumed to predominate, decreases sharply with increase of C_o from 30 to 180 mg/l, then at higher initial MB concentrations (above 180 mg/l) the values of k_s are almost constant. The decrease of k_s with increasing C_o is in agreement with the trend of k_1 and k_2 predicted from Lagergren's model and the pseudo-second-order model shown in Table 1.

In order to confirm the above conclusions about the actual rate controlling steps in MB adsorption on BBP, the experimental data was also analyzed by the expression of Boyd et al. [36]:

$$F = 1 - \frac{6}{\pi^2}\exp(-BT) \tag{12}$$

where F is the fractional attainment of equilibrium, at different times, t, and Bt is a function of F.

$$F = \frac{q_t}{q_e} \tag{13}$$

where q_t and q_e are the dye uptake (mg/g) at time t and at equilibrium, respectively.Eq. (12) can be rearranged to

$$\mathrm{Bt} = -0.4977 - \ln(1 - F) \tag{14}$$

The values of Bt were calculated from Eq. (14) and plotted against time as shown in Fig. 8. The plots are linear in the initial period of adsorption and do not pass through the origin but have intercept values close to −0.4977, indicating that external mass transfer is the rate limiting process in the beginning of adsorption. The calculated values of B were used to determine

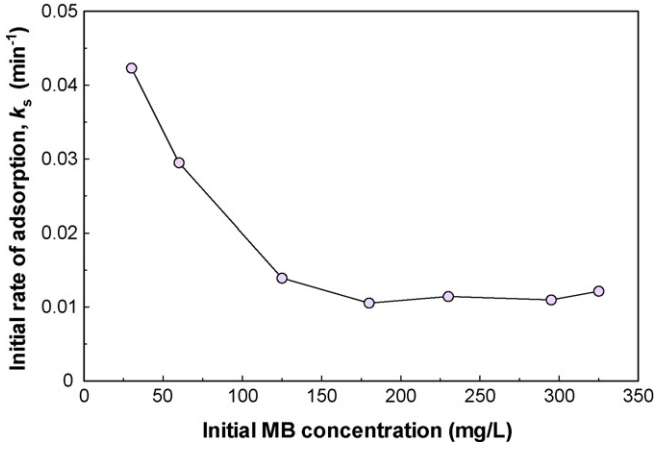

Fig. 7. Plots of the rate constant of external mass transfer, k_s, vs. C_o for the initial stage of adsorption at 30 °C and different initial MB concentrations (BBP dose: 1.5 g/l).

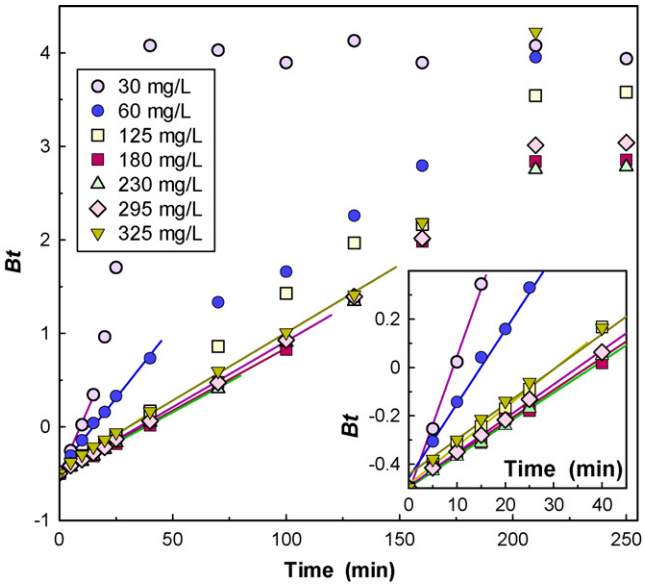

Fig. 8. Boyd plots for MB adsorption at 30 °C and different initial MB concentrations (BBP dose: 1.5 g/l).

the effective diffusion coefficient, D_i, (cm^2/s) from the equation:

$$B = \frac{\pi^2 D_i}{r^2} \tag{15}$$

where r is the radius of the adsorbent particle assuming spherical shape. The values of D_i in Table 2 show that the relation between C_o and the effective diffusion coefficient, D_i, has the same general trend as the intercept, c, obtained from the pore diffusion calculations. This trend is probably caused by the increased dimerization of MB with the increase of its concentration in solution [37,38]. Also, by examining Fig. 7, it can be seen that the initial period where external mass transfer is the rate controlling step increases from 15 to 150 min when C_o increases from 30 to 323 mg/l. The discrepancies in the film-diffusion period (Table 2) calculated from the pore diffusion equation and the Boyd equation are probably due to two reasons: the first reason is the distortion of the experimental-error distribution with the transformations in the X and Y axis, leading to some bias in the piecewise linear regression results [39], and the second reason is the wide time gaps between experimental data points in the mid range of adsorption (30 min gaps) making it difficult to obtain an accurate estimate of the time where film-diffusion control ends.

3.3. Equilibrium studies

3.3.1. Effect of solution pH on dye uptake

The effect of initial pH on equilibrium sorption capacity of BBP was studied at 60 mg/l initial MB concentration and at 30 °C. It was observed that the solution pH affects the amount of dye adsorbed. As seen from Fig. 9, the sorption of MB was minimum at the initial pH 2, increased with pH up to 4 and then remained nearly constant. At higher pH, the BBP may become negatively charged, which enhances the positively charged dye cations through electrostatic forces of attraction [21]. This finding is similar to that made in previous works on adsorption

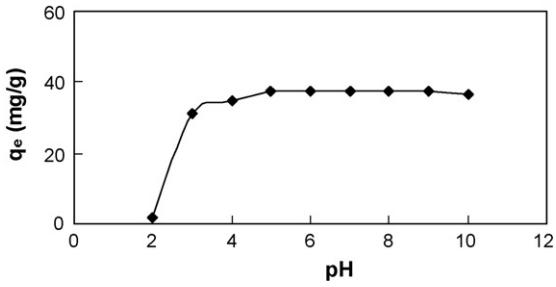

Fig. 9. Effect of pH on equilibrium uptake of MB (BBP dose: 1.5 g/l; C_0: 60 mg/l).

[40–42]. Over the pH ranges of 4–10, the dye adsorption at equilibrium was almost constant. The fact that the MB sorption rate on the BBP was low at lower pH may be because the surface charge may become positively charged, thus making H^+ ions compete effectively with dye cations, causing a decrease in the amount of dye adsorbed. A similar behavior was observed for biosorption of MB by *Posidonia oceanica* (L.) fibres [21].

3.3.2. Equilibrium modeling

Although there are many adsorption isotherms in the literature, the most widely used by are Freundlich [43] and Langmuir [44] isotherms. The Freundlich isotherm can be used for non-ideal adsorption on heterogeneous surfaces. The heterogeneity arises from the presence of different functional groups on the surface, and/or various adsorbent–adsorbate interactions. The Freundlich isotherm is expressed by the following empirical equation:

$$q_e = K_F C_e^{1/n} \tag{16}$$

where K_F is the Freundlich adsorption constant ($(mg/g)(l/g)^n$) and $1/n$ is a measure of the adsorption intensity.

The development of the Langmuir isotherm assumes monolayer adsorption on a homogenous surface. It is expressed by the following equation:

$$q_e = \frac{q_m K_a C_e}{1 + K_a C_e} \tag{17}$$

where C_e is the equilibrium concentration (mg/l), q_e the amount adsorbed (mg/g), q_m is q_e for complete monolayer adsorption capacity (mg/g), and K_a is the equilibrium adsorption constant (l/mg).

The experimental equilibrium results were fitted by non-linear regression to the Freundlich and Langmuir isotherm models. Fig. 10 and Table 3 show that the Langmuir isotherm gives a better fitting to the experimental results ($R^2 = 0.9749$) than the Freundlich isotherm ($R^2 = 0.9677$) which suggests that

Table 3
Isotherm constants for MB sorption on BBP at 30 °C

Langmuir isotherm			Freundlich isotherm		
q_m (mg/g)	K_a (l/mg)	R^2	K_f ((mg/g)(l/g)^n)	n	R^2
192.7	0.07145	0.9749	27.83	2.345	0.9677

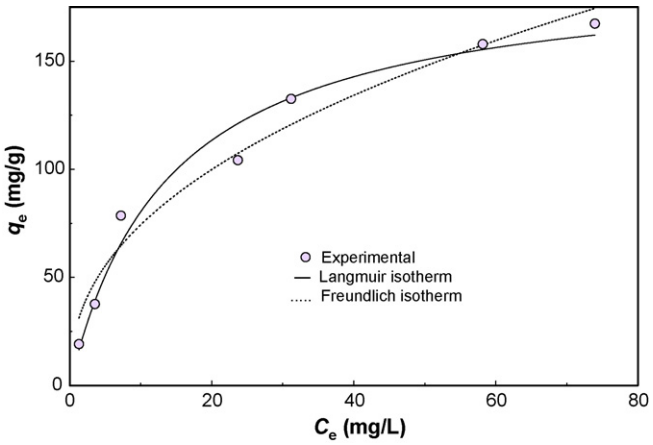

Fig. 10. Isotherm plots for MB sorption on BBP at 30 °C (BBP dose: 1.5 g/l).

adsorption takes place by monolayer adsorption on a homogeneous surface.

3.3.3. Comparison of various low-cost adsorbents

Table 4 compares the adsorption capacity of different types of adsorbents used for removal of MB. The most important parameter to compare is the Langmuir q_m value since it is a measure of adsorption capacity of the adsorbent. The value of q_m in this study is larger than those in most of previous works. This suggests that MB could be easily adsorbed on BBP.

3.4. Characterization of BBP

The surface structure of BBP was analyzed by scanning electronic microscopy (SEM) before and after MB sorption (Fig. 11a and b). The textural structure examination of BBP particles can be observed from the SEM photographs at 500× magnification (Fig. 11a). This figure reveals that the BBP particles were mostly irregular in shape and porous. After dye adsorption, a significant change is observed in structure of the BBP (Fig. 11b). It can be seen that the BBP surface became rough because it is covered by dye molecules.

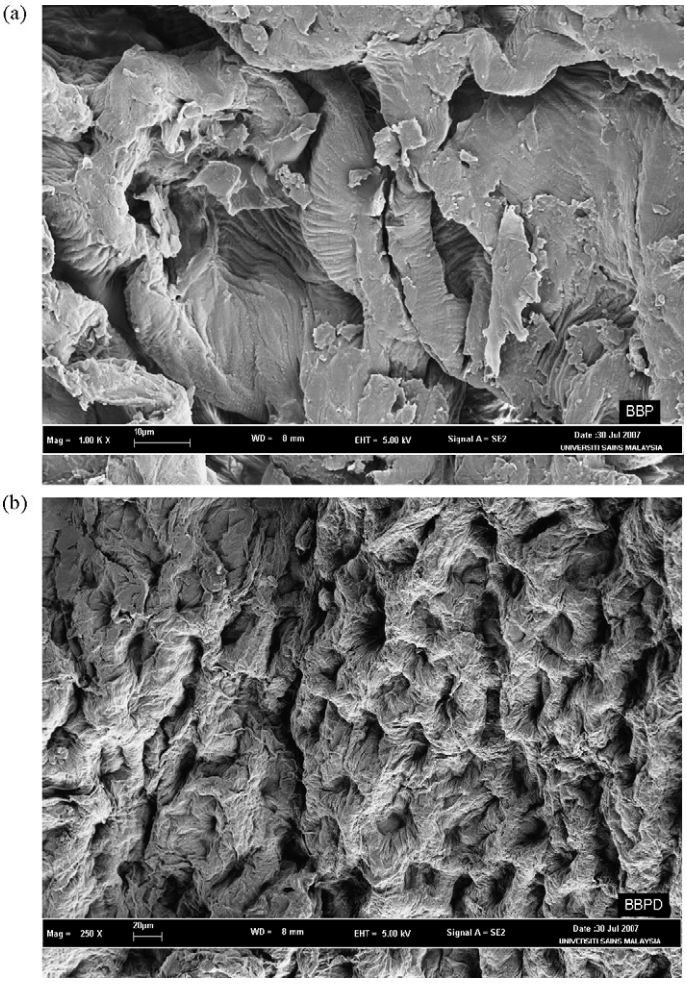

Fig. 11. Typical SEM micrograph of BBP particle (magnification: 1000): (a) before dye adsorption and (b) with dye adsorbed.

Table 4
Comparison of adsorption capacities of various adsorbents for methelene blue

Adsorbent	q_m (mg/g)	T (°C)	Reference
Broad bean peels (BBP)	192.7	30	This work
Caulerpa racemosa var. *cylindracea*	3.423	27	[45]
Dehydrated peanut hull	123.5	30	[46]
Sulphuric acid treated *Parthenium* (SWC)	39.68	26 ± 1	[47]
Phosphoric acid treated *Parthenium* (PWC).	88.49	26 ± 1	[47]
Banana peel	20.8	30	[48]
Orange peel	18.6	30	[48]
Neem (*Azadirachta indica*) leaf powder	8.76	27	[49]
Cedar sawdust	142.36	20	[50]
Crushed brick	96.61	20	[50]
Algae *Gelidium*	171	20	[51]
Algal waste	104	20	[51]
Composite material	74	20	[51]

4. Conclusions

1. The present study shows that the broad been peels, an abundant agricultural waste, can be used as sorbent for the removal of methylene dye from aqueous solutions.
2. The amount of dye sorbed was found to vary with initial methylene blue concentration and contact time.
3. The sorption equilibrium data were found to fit the Langmuir isotherm, indicating monolayer adsorption on a homogenous surface.
4. Lagergren's pseudo-first-order model can be used to predict the adsorption kinetics.
5. The overall rate of dye uptake was found to be controlled by external mass transfer at the beginning of adsorption, while intraparticle-diffusion controlled the overall rate of adsorption at a later stage.

References

[1] G. Mishra, M. Tripathy, A critical review of the treatment for decolourization of textile effluent, Colourage 40 (1993) 35–38.

[2] Y. Fu, T. Viraraghavan, Fungal decolourization of wastewaters: a review, Bioresour. Technol. 79 (2001) 251–262.

[3] E.A. Clarke, R. Anliker, Organic dyes and pigments Handbook of Environmental Chemistry, Anthropogenic Compounds, vol.3, part A, Springer-Verlag, New York, 1980, pp. 181–215.

[4] I.M. Banat, P. Nigam, D. Singh, R. Marchant, Microbial decolourization of textile-dye containing effluents: a review, Bioresour. Technol. 58 (1996) 217–227.

[5] A.K. Mittal, S.K. Gupta, Biosorption of cationic dyes by dead macro fungus *Fomitopsis carnea*: batch studies, Water Sci Technol. 34 (1996) 157–181.

[6] H.C. Chu, K.M. Chen, Reuse of activated sludge biomass. I. Removal of basic dyes from wastewater by biomass, Process Biochem. 37 (2002) 595–600.

[7] Y. Fu, T. Viraraghavan, Removal of Congo Red from an aqueous solution by fungus *Aspergillus niger*, Adv. Environ. Res. 7 (2002) 239–247.

[8] H. Zollinger, Azo dyes and pigments, in: Colour Chemistry-Synthesis, Properties and Applications of Organic Dyes and Pigments, VCH, New York, 1987, pp. 92–100.

[9] T. Robinson, G. Mcmullan, R. Marchant, P. Nigam, Remediation of dyes in textile effluent: a critical review on current treatment technologies with a proposed alternative, Bioresour. Technol. 77 (2001) 247–255.

[10] O.J. Hao, H. Kim, P.C. Chiang, Decolorization of wastewater, Crit. Rev. Environ. Sci. Technol. 30 (2000) 449–502.

[11] B.H. Hameed, A.T.M. Din, A.L. Ahmad, Adsorption of methylene blue onto bamboo-based activated carbon: kinetics and equilibrium studies, J. Hazard. Mater. 141 (2007) 819–825.

[12] I.A.W. Tan, B.H. Hameed, A.L. Ahmad, Equilibrium and kinetic studies on basic dye adsorption by oil palm fibre activated carbon, Chem. Eng. J. 127 (2007) 111–119.

[13] B.H. Hameed, A.L. Ahmad, K.N.A. Latiff, Adsorption of basic dye (methylene blue) onto activated carbon prepared from rattan sawdust, Dyes Pigments 75 (2007) 143–149.

[14] I.A.W. Tan, A.L. Ahmad, B.H. Hameed, Optimization of preparation conditions for activated carbons from coconut husk using response surface methodology, Chem. Eng. J. 137 (2008) 462–470.

[15] B.H. Hameed, F.B.M. Daud, Adsorption studies of basic dye on activated carbon derived from agricultural waste: *Hevea brasiliensis* seed coat, Chem. Eng. J. 139 (2008) 48–55.

[16] Z. Aksu, İ. Alper İşoğlu, Removal of copper (II) ions from aqueous solution by biosorption onto agricultural waste sugar beet pulp, Process Biochem. 40 (2005) 3031–3044.

[17] C.H. Weng, Y.F. Pan, Adsorption of a cationic dye (methylene blue) onto spent activated clay, J. Hazard. Mater. 144 (2007) 355–362.

[18] A.A. Ahmad, B.H. Hameed, N. Aziz, Adsorption of direct dye on palm ash: Kinetic and equilibrium modeling, J. Hazard. Mater. 141 (2007) 70–76.

[19] M. Hasan, A.L. Ahmad, B.H. Hameed, Adsorption of reactive dye onto crosslinked chitosan/oil palm ash composite beads, Chem. Eng. J. 136 (2008) 164–172.

[20] Z. AL-Qoda, Adsorption of dyes using shale oil ash, Water Res. 34 (2000) 4295–4303.

[21] M.C. Ncibi, B. Mahjoub, M. Seffen, Kinetic and equilibrium studies of methylene blue biosorption by *Posidonia oceanica* (L.) fibres, J. Hazard. Mater. B139 (2007) 280–285.

[22] A.E. Ofomaja, Y.S. Ho, Equilibrium sorption of anionic dye from aqueous solution by palm kernel fibre as sorbent, Dyes Pigments 74 (2007) 60–66.

[23] S.B. Bukallah, M.A. Rauf, S.S. AlAli, Removal of methylene blue from aqueous solution by adsorption on sand, Dyes Pigments 74 (2007) 85–87.

[24] M.I. El-Khaiary, Kinetics and mechanism of adsorption of methylene blue from aqueous solution by nitric-acid treated water-hyacinth, J. Hazard. Mater. 147 (2007) 28–36.

[25] E. De Miquel Gordillo, in: El Garbanzo (Ed.), Una alternativa para el secano, Mundi-Prens, Madrid, 1991.

[26] M.T. Al-Kaisey, H. Jaddou, S.R. Alani, A.A.K. Hussain, Production of cereal based of powdered baby food, Sci. J. Iraqi Atom. Energy Commun. 2 (2000) 149–154.

[27] M.T. Macarulla, C. Medina, M. Aránzazu De Diego, M. Chávarri, A.M. Zulet, J.A. Martínez, C. Nöel-Suberville, P. Higueret, M.P. Portillo, Effects of the whole seed and a protein isolate of faba bean (*Vicia faba)* on the cholesterol metabolism of hypercholesterolaemic rats, Br. J. Nutr. 85 (2001) 607–614.

[28] S. Lagergren, Zur theorie der sogenannten adsorption geloster stoffe. 591. Kungliga Svenska Vetenskapsakademiens, Handlingar 24 (4) (1898) 1–39.

[29] Y.S. Ho, Adsorption of heavy metals from waste streams by peat, Ph.D. thesis, University of Birmingham, Birmingham, U.K., 1995.

[30] J. Hintze, *NCSS, PASS, and GESS*. Kaysville, Utah: NCSS (2006).

[31] D. Mohan, K.P. Singh, Single and multicomponent adsorption of cadmium and zinc using activated carbon derived from bagasse—an agricultural waste, Water Res. 36 (2004) 2304–2318.

[32] W.J. Weber Jr., J.C. Morris, Kinetics of adsorption on carbon from solution, J. Sanitary Eng. Div. Proceed. Am. Soc. Civil Eng. 89 (1963) 31–59.

[33] Y.S. Ho, G. McKay, The kinetics of sorption of basic dyes from aqueous solution by sphagnum moss peat, Can. J. Chem. Eng. 76 (1998) 822–827.

[34] J. Bujdak, P. Komadel, Interaction of methylene blue with reduced charge montmorillonite, J. Phys. Chem. B 101 (1997) 9065–9068.

[35] A.P.P. Cione, M.G. Neumann, F. Gessner, Time-dependent spectrophotometric study of the interaction of basic dyes with clays: III. Mixed dye aggregates on SWy-1 and Laponite, J. Colloid Interf. Sci. 198 (1998) 106–112.

[36] G.E. Boyd, A.W. Adamson, L.S. Myers Jr., The exchange adsorption of ions from aqueous solutions by organic zeolites, II: kinetics, J. Am. Chem. Soc. 69 (1947) 2836–2848.

[37] N. Strataki, V. Bekiari, P. Lianos, Study of the conditions affecting dye adsorption on titania films and of their effect on dye photodegradation rates, J. Hazard. Mater. 146 (2007) 514–519.

[38] R.N. Muir, A.J. Alexander, Structure of monolayer dye films studied by Brewster angle cavity ringdown spectroscopy, Phys. Chem. 5 (2003) 1279–1283.

[39] H. Motulsky, A. Christopoulos, Fitting Models to Biological Data Using Linear and Nonlinear Regression, Oxford University Press, Oxford, 2004.

[40] P. Waranusantigul, P. Pokethitiyook, M. Kruatrachue, E.S. Upatham, Kinetics of basic dye (methylene blue) biosorption by giant duckweed (*Spirodela polyrrhiza*), Environ. Pollut. 125 (2003) 385–392.

[41] Y. Bulut, H. Aydın, A kinetics and thermodynamics study of methylene blue adsorption on wheat shells, Desalination 194 (2006) 259–267.

[42] R. Han, Y. Wang, P. Han, J. Shi, J. Yang, Y. Lu, Removal of methylene blue from aqueous solution by chaff in batch mode, J. Hazard. Mater. B137 (2006) 550–557.

[43] H.M.F. Freundlich, Uber Die Adsorption in Losungen. Zeitschrift fur Physikalische Chemie 57 (1906) 385.

[44] I. Langmuir, Constitution and fundamental properties of solids and liquids. I. Solids, J. Am. Chem. Soc. 38 (11) (1916) 2221.

[45] S. Cengiz, L. Cavas, Removal of methylene blue by invasive marine seaweed: *Caulerpa racemosa* var. *Cylindracea*, Bioresour. Technol. 99 (2008) 2357–2363.

[46] D. Özer, G. Dursun, A. Özer, Methylene blue adsorption from aqueous solution by dehydrated peanut hull, J. Hazard. Mater. 144 (2007) 171–179.

[47] H. Lata, V.K. Garg, R.K. Gupta, Removal of a basic dye from aqueous solution by adsorption using *Parthenium hysterophorus*: an agricultural waste, Dyes Pigments 74 (2007) 653–658.

[48] G. Annadurai, R.S. Juang, D.J. Lee, Use of cellulose-based wastes for adsorption of dyes from aqueous solutions, J. Hazard. Mater. B92 (2002) 263–274.

[49] K.G. Bhattacharyya, A. Sharma, Kinetics and thermodynamics of methylene blue adsorption on neem (*Azadirachta indica*) leaf powder, Dyes Pigments 65 (2005) 51–59.

[50] O. Hamdaoui, Batch study of liquid-phase adsorption of methylene blue using cedar sawdust and crushed brick, J. Hazard. Mater. B135 (2006) 264–273.

[51] V.J.P. Vilar, C.M.S. Botelho, R.A.R. Boaventura, Methylene blue adsorption by algal biomass based materials: biosorbents characterization and process behaviour, J. Hazard. Mater. 147 (2007) 120–132.